

# MECHANICAL CHARACTERIZATION OF SURFACE MICROMACHINED HOLLOW METALLIC MICRONEEDLES

Shankar Chandrasekaran and A. Bruno Frazier

School of Electrical and Computer Engineering  
Georgia Institute of Technology  
Atlanta, GA 30332-0250

**Abstract** - This paper will report on the mechanical characterization of hollow metallic microneedles. The characterization will include the effects of design variations on the buckling and penetration force of these microneedles, and on the fluid flow characteristics. Needles of five different tip geometry and three different taper angles were designed. The taper angle varies between 15° and 30°. The lengths of the needle shaft tested were 500 μm, 1000 μm and 1500 μm respectively. Microneedles were fabricated using an extension of the work reported earlier. A simple horizontal loading set up consisting of a load cell and a micromanipulator was designed. A rigid orthogonal surface was used in order to study the buckling force, while a mechanically “skin-like” material was used to determine the penetration force. The buckling force was found to vary between 54 gF and 100 gF for needles with shaft lengths of 1500 and 500 μm, respectively. The penetration force was found to be independent of shaft length and was approximately 8 gF. While the needle tips with 15° taper angle failed, the needles with 20° taper angle performed better but experienced a 50% tip failure rate. The flow rate of the microneedles was characterized over a range of 0 – 100 psi using distilled water and air as the fluid media.

**Keywords:** Microneedles, mechanical characterization

## I. INTRODUCTION

Over the last few years significant work [1-7] has been done on the development of micromachining processes for the fabrication of microneedles. Towards this end, technologies have been established for realizing microneedles using various materials including silicon, metals and polymers. Microneedles offer several advantages when compared to conventional needle technologies including being minimally invasive due to their small cross-sectional area, providing precise penetration depth under the skin, inducing minimal trauma during insertion due to the

advanced tip designs, and increased functionality (e.g., addition of fluid mixers, multiple lumens, multiple fluid delivery ports). Additionally, with the development of microfluidic systems, microneedles could serve as a low dead volume, highly functional interfacing technology between miniaturized bioanalytical systems and patients under study. Besides drug delivery, microneedles have found use as ultrasonic cutters [8], ultrasonic atomizers [9] and surgical device [10]. Consequently, there is an increasing interest in developing methodologies for fabricating microneedles as well as characterizing the resulting microneedles.

The majority of the previously reported work on microneedles has been using silicon as the primary material of construction. However, due to the brittle nature of silicon, additional supporting materials have been explored in order to improve the performance of composite ‘silicon’ microneedles [11]. Metallic microneedles have gained considerable interest because of the range of materials available and ease of fabrication by micromolding and electroforming. Allen *et al.* reported one of the earliest works with information on the mechanical characterization of microneedles. The work demonstrated the use of microneedles for transdermal drug delivery and was found to enhance transdermal transport. However, quantitative information on the penetration force for the needle insertion was not reported. The common reported modes of failure in microneedles include fracture, buckling during insertion, and poor adhesion between the structural parts of the microneedle. Other critical performance criteria for microneedles include having the capability of withstanding the fluidic pressure exerted on the walls during fluid injection / extraction and elimination of clogging at the orifices and along the microneedle lumen(s).

This work represents the first report focused on the characterization of microneedles for their fluidic and mechanical properties. The following sections will give a brief description of the fabrication process, establish the experimental methodology for characterizing the microneedles, and present results and conclusions.

## II. METHODS

### A. Design of Microneedles

Understanding skin anatomy is critical in the design of the microneedles. The primary objective of these minimally invasive microneedles is to facilitate pain-free drug delivery. The human skin is made of three layers: the outer skin which is made of dead tissues; the viable epidermis, a tissue of living cells, which has a thickness up to 100  $\mu\text{m}$ ; and the underlying dermis. This requires that the needle be long enough to penetrate through these layers in order to reach the sub-cutaneous layers, capillaries and larger blood vessels. Based on this, microneedles of different shaft lengths (200 $\mu\text{m}$ , 500 $\mu\text{m}$ , 1000 $\mu\text{m}$  and 1500 $\mu\text{m}$ ) were designed for the purpose of the study. Buckling is the expected mode of failure in electroformed metal structures as long as the metals are electroplated within the standard operating range. The other factor that is of importance, particularly, in determining the penetration force is the tip geometry. Sharper needle tips can be expected to require less force for insertion, but the reduced penetration force comes at the expense of reduced strength near the tip. Needle tips with three different taper designs were fabricated and characterized in order to study the effects of geometry on the microneedle penetration force. The penetration studies were performed using a skin-like polymer material known to have similar penetration characteristics as skin (PS-4B, M-line Accessories Inc.).

### B. Fabrication Approach

The microneedles were fabricated using a previously established and reported [12, 13, 14] low temperature IC compatible surface micromachining process. The process allowed for fabrication of the microneedles on many substrates including silicon, plastic and glass. Additionally, the substrates were not consumed in the fabrication process and could be re-used. To begin, three thin films of metal were physical vapor deposited onto the substrate. In sequential deposition order, the layers included an adhesion layer (to provide mechanical adhesion between the substrate and overlying electroplating seed layer), an electroplating seed layer to facilitate electroplating onto the surface, and an overlying protective layer to prevent oxidation / contamination of the seed layer during processing leading up to the electroplating process. Next, a 40 $\mu\text{m}$  thick layer of photoresist (Clariant AZ4620) was spun on top of the 'seed layers' and patterned to define the micromolds for the bottom wall of the microneedle shafts. Subsequently, 35  $\mu\text{m}$  of palladium was electroplated into the micromolds. The choice of the material was based on the mechanical properties and the biologically inert characteristic of electroplated palladium [15, 16, 17]. Besides palladium,

microneedles were fabricated using nickel, a palladium-cobalt alloy, and gold. In the case of nickel, a thin layer of gold was deposited on the surface in order to address the biocompatibility issues for biomedical applications. Subsequent to electroplating the bottom wall, a 40  $\mu\text{m}$  thick photoresist layer was deposited and patterned to define the inner lumen of the microneedles. A 1500  $\text{\AA}$  gold layer was sputtered onto the photoresists layer. The gold layer served as the electroplating seed layer during formation of the top shell. Next, a 30 micrometer thick photoresist layer was spun and patterned to define the micromold for the top wall of the microneedle shafts and the structural side bars of the needle arrays. Subsequently, a 25  $\mu\text{m}$  thick palladium layer was electroplated through the micromold to form the top wall and the structural sidebars. In a batch process, the microneedles and arrays were released from the substrate by etching the underlying gold layer. Next, the photoresist layer that defines the inner lumen was removed by dissolving it in an acetone bath for 12 hours, followed by a methanol/isopropanol rinse and a de-ionized water rinse, thus producing a hollow lumen. After clearing the microneedle lumens, the adhesion and seed layers were removed from the bottom-side of the microneedles.

### C. Experiment Setup: Penetration Force and Buckling Force Studies

A horizontal loading setup was used for the purpose of the penetration force and buckling force studies. The test platform consisted of a load cell connected to a rigid steel platform, and horizontal translator controlled by a micromanipulator to force the needle against the load cell. The needle was attached to an aluminum block using an epoxy material. The load cell (LCGC-500G, Omega Engineering Inc.) was capable of measuring load up to 500 g upon application of a 10 V external excitation voltage. The sensitivity of the device was  $\pm 0.2$  g. The load cell was interfaced with LabView to obtain real time data upon forcing the needle against loading surface. A skin-like material was used to determine the penetration force. The material had a Young's Modulus of 200 psi. This material was rigidly attached to the load cell platform.

### D. Experimental Setup: Fluid Flow Rate vs. Pressure Studies

The experimental setup for the fluid flow rate studies consisted of a pressure transducer (PX182 100GV, Omega Engineering Inc.) mounted at the inlet of the microneedle lumen (used to determine the inlet pressure), and a syringe pump (100, KD Scientific) to control the fluid flow rate. The pressure transducer was capable of measuring up to 100 psi with a resolution of  $\pm 0.003$  psi. The microneedle was affixed to the testing jig using an epoxy material.

### III. RESULTS AND DISCUSSION

The hollow metallic microneedles were fabricated using the process described in the previous section. Figure 1 is an scanning electron micrograph (SEM) of a typical five-needle array with the center-to-center separation distance of 2.00 mm. The length of the shaft beyond the cross-sectional sidebars is 500 micrometers. The top port is  $45 \times 45 \mu\text{m}^2$  while the bottom port is  $75 \times 75 \mu\text{m}^2$ . A mechanical barb, which serves to hold the microneedle in place after penetration, is also shown in the figure. The barb extends 50 micrometers perpendicular to the length of the needle and 250 micrometers along the length of the needle. The tip of the needle is 10 micrometers in width. The taper angle of the tip is  $20^\circ$ . The metal reinforcement, which was added to reduce the stress at the junction between the needle shaft and the cross-sectional sidebars, can be seen. The width of the needle at the distal end of the needle is  $300 \mu\text{m}$ , while that at the proximal end is 85 micrometers. The  $300 \mu\text{m}$  wide lumen helps minimize the pressure along the bulk of the fluid path. The micro rivets designed along the length of the shaft are  $10 \times 20 \mu\text{m}^2$ . The thickness of the tip is  $25 \mu\text{m}$ , while the thickness of the bottom wall is  $35 \mu\text{m}$ . The width of the tip of the needle for a  $15^\circ$  taper is 6 micrometers.

Buckling tests were performed on the needles of three different shaft lengths,  $500 \mu\text{m}$ ,  $1000 \mu\text{m}$  and  $1500 \mu\text{m}$ , respectively. The buckling force was measured by forcing the needle against a rigid metal surface, which was affixed to the load cell. The average buckling force based on the collected data was found to be 100 gram Force (gF). The standard deviation is 6gF. The buckling force was found to vary between 93gF to 110gF for a needle of length  $500 \mu\text{m}$ . Figure 2 is a plot of buckling force on needles of different shaft lengths vs. the microneedle shaft length. As expected the buckling force increases with decreasing shaft length.

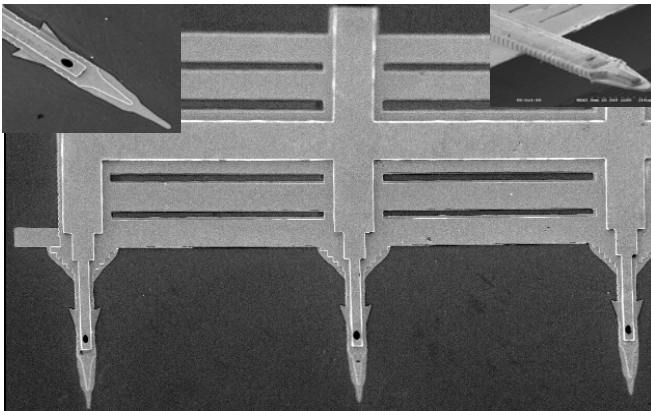


Fig. 1. SEM micrograph of three needles in a five -needle array. Insert: Insert shows a higher magnification of two different needle designs.

The penetration force was determined by forcing the needle against a skin-like material (photoelastic sheet PS-4B). The penetration tests were performed on needles of different lengths as well as needles of different tapering angle,  $15^\circ$ ,  $20^\circ$  and  $30^\circ$  respectively in order to study the effect of length as well as the taper angle on the penetration force. Figure 3, is a plot of real time distribution of the force on the needle vs. time. The peak represents the penetration force, which is 8.47gF for a needle of length  $1500 \mu\text{m}$ . The average penetration force for needles of length  $500 \mu\text{m}$ ,  $1000 \mu\text{m}$ , and  $1500 \mu\text{m}$  are 8gF, 9gF, and 10gF respectively. Less than 5% of the needles that were tested with the taper angle of  $30^\circ$  failed due to fracture of the tip.

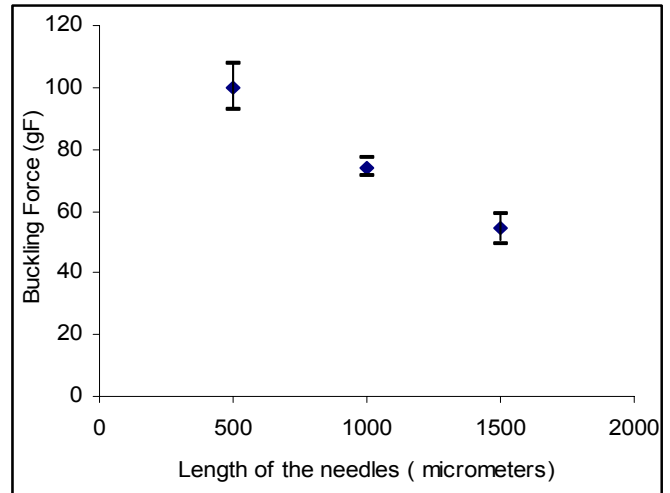


Fig 2. Buckling force vs. length of the needle along with the standard deviation. The standard deviation was found to vary between 7 gF for a needle of length  $500 \mu\text{m}$  and 3 gF for needle of length  $1500 \mu\text{m}$ .

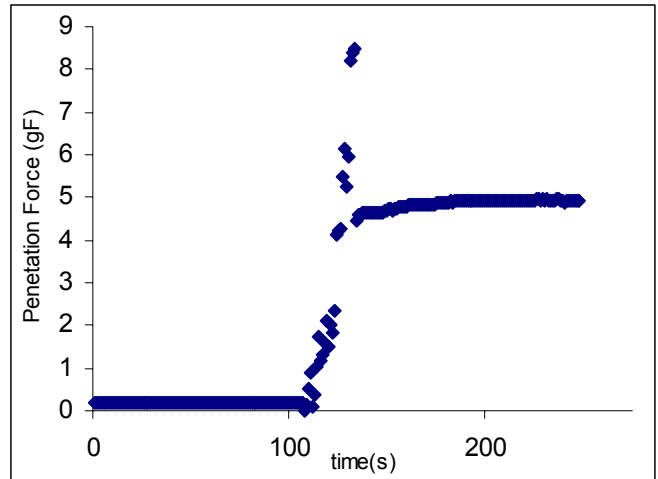


Fig 3. Real-time distribution of force as the needle is forced into the skin-like material. The peak represents the maximum force that is required to force the needle through the material.

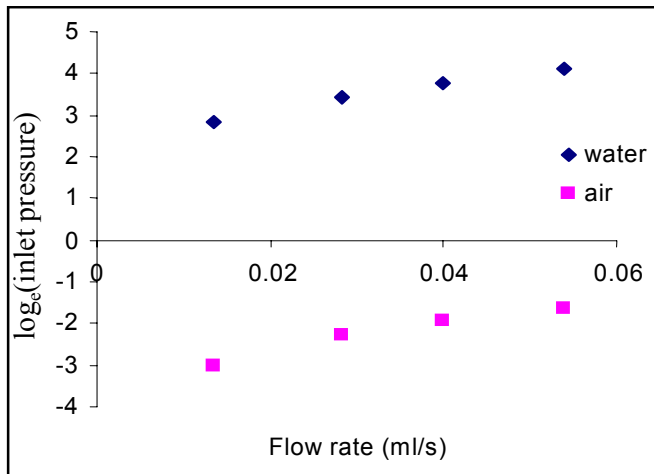


Fig. 4. Flow rate vs  $\log_e$  (inlet pressure) for both air and water.

Tests were also performed on the needles of various taper angles. Preliminary results on tip of taper angle  $20^\circ$  indicate that the penetration force is lesser but the failure rate at the tip is high. The needles with taper angle of  $15^\circ$  buckled and did not penetrate through the skin-like material. More experiments need to be performed to confirm the trend. The force required for penetration was found to be 8% of the buckling force for a microneedle of shaft length  $500 \mu\text{m}$  and 18% for a microneedle of length  $1500 \mu\text{m}$ , both with a taper angle of  $30^\circ$ . This clearly demonstrates the feasibility of these microneedles for the purpose of drug delivery and biofluid extraction.

Fluidic tests were performed on the microneedles with a shaft length of  $1000 \mu\text{m}$  using the procedure described in the previous section. The inlet pressure required to establish flow rates ranging from  $0.014 \text{ ml/s}$  to  $0.67 \text{ ml/s}$  were determined for both air and water. The pressure required was found to vary between  $49 \text{ Pa}$  for a flow rate of  $0.014 \text{ ml/s}$  to  $243 \text{ Pa}$  for a flow of  $0.068 \text{ ml/s}$  for air, Figure 4 shows a plot of inlet pressure vs. the flow rates for both air and water. For water, an average pressure of  $3.0 \text{ KPa}$  was required for a flow rate of  $0.017 \text{ ml/s}$ ,  $5.8 \text{ KPa}$  for a flow rate of  $0.034 \text{ ml/s}$ , and  $12.1 \text{ KPa}$  for a flow rate of  $0.67 \text{ ml/s}$ .

#### IV. CONCLUSION

Surface micromachining technology was used to fabricate microneedles of various tip geometries. Penetration and buckling tests were performed on these needles. The microneedles with a tip taper angle of  $30^\circ$  were found to be the most robust for the purpose of insertion. While the other taper angles yielded lesser penetration force, they were not reliable and hence not suitable for practical applications. Fluidic studies demonstrated that flow rates of the order of  $0.067 \text{ ml/s}$  are possible at reasonable applied pressures. The

microneedle was capable of withstanding as high as  $12 \text{ KPa}$  without failure due to delamination (i.e., leakage). Based on the above results, the ideal geometry for minimally invasive microneedles for pain free drug delivery has been established. The mechanical characterization studies demonstrate that the microneedles are mechanically strong enough to penetrate the skin-like material without failure due to buckling by a factor of approximately 10.

#### ACKNOWLEDGMENTS

The authors of this work would like to thank Becton Dickinson Technologies, Clariant Corporation, Lucent Technologies for support of this work.

#### REFERENCES

- [1] John D. Brazzle, Ian Papautsky, and A. Bruno Frazier, "Fluid-coupled metallic microfabricated needle arrays," in *Proc. SPIE Micro Fluidic Devices and Systems*, Santa Clara, CA, Sep. 21-24, pp. 116-124, 1998.
- [2] Surface Micromachined Microneedles. Inventors: A. Bruno Frazier, and John D. Brazzle. U.S. Patent No. 5,876,582. Date of Issue: September 27, 1999.
- [3] S. Henry, D.V. McAllister, M.G. Allen, and M.R. Prausnitz, "Micromachined needles for the transdermal delivery of drugs", in *IEEE Micro Electro Mechanical Systems Conf.*, Heidelberg, Germany, Jan. 25-29, 1998.
- [4] L. Lin, A.P. Pisano, R.S. Muller, "Silicon processed microneedles," in *Proc. Transducers' 93*, Yokohama, Japan, June 7-10, pp. 237-240, 1993.
- [5] D.V. McAllister, F. Cros, S.P. Davis, L.M. Matta, M.R. Prausnitz, and M.G. Allen, "Three-dimensional hollow microneedle and microtube arrays," in *Proc. Transducers' 99*, Sendai, Japan, June 7-10, pp. 1098-1101, 1999.
- [6] Liwei Lin and Albert P. Pisano, "Silicon-processed microneedles," *IEEE Journal of Microelectromechanical Systems*, Vol. 8, No. 1, pp. 78-84, 1999.
- [7] N.H. Talbot and A.P. Pisano, "Polymolding: two wafer polysilicon micromolding of closed-flow passages for microneedles and microfluidic devices," in *IEEE Tech. Dig. Solid-State Sensor and Actuator Workshop*, Hilton Head, SC, June 8-11, pp. 265-268, 1998.
- [8] A. Lal, R. M. White, "Silicon micromachined ultrasonic micro-cutter," *IEEE Proceedings of Ultrasonic Symposium*, Vol. 3, pp. 1907-1911, 1994
- [9] A. Lal, R. M. White, "Micromachined Silicon needle for ultrasonic surgery," *IEEE Proceedings of Ultrasonic Symposium*, Vol. 2, pp. 1593-1596, 1995
- [10] A. Lal, R. M. White, "Micromachined Silicon ultrasonic atomizer," *IEEE Proceedings of Ultrasonic Symposium*, Vol. 1, pp. 339-342, 1996
- [11] Phillip A. Stupar and Albert P. Pisano, "Silicon, Parylene and Silicon/Parylene Micro-Needles for Strength

and Toughness," in *Proc. Transducers '01*, Munich, Germany, June 10-14, pp. 2001.

[12] I. Papautsky, J. Brazzle, H. Swerdlow, and A.B. Frazier, "A Low Temperature, IC Compatible Process for Fabricating Surface Micromachined Metallic Microchannels", *IEEE Journal of Microelectromechanical Systems*, (7) 267-73 (1998).

[13] I. Papautsky, H. Swerdlow, and A.B. Frazier, "Surface Micromachined IC Compatible Technology for Fabricating Metallic MicroChannels", *10th IEEE International Workshop on Micro Electro Mechanical Systems*, Nagoya, Japan, January, 1997, pp. 104-109.

[14] J. Brazzle, I. Papautsky, and A.B. Frazier, "Fluid-coupled metallic micromachined needle arrays," in *Proc. 20th International Conference of the IEEE Engineering in Medicine and Biology Society (EMBS '98)*, Hong Kong, Oct. 29 – Nov. 1, pp. 1837-1840, 1998.

[15] J. Black, *Biological performance of materials: Fundamentals of biocompatibility*, Marcel Dekker, New York, 1992.

[16] S. D. Cramer and D. Schlain, "Electrodeposition of palladium and platinum from aqueous electrolytes," *Plating*, May, pp. 516-522, 1969.[17] E. J. Kudrak, J. A. Abys, H. K. Straschil, I. Kadija, and J. J. Maisano, "Palladium and palladium alloy plating for the 90's," presented at *Connectors '93*, East Midlands, England, May 19, 1993.